

# A Reevaluation of the Structure of Purified Tubulin in Solution: Evidence for the Prevalence of Oligomers over Dimers at Room Temperature

N. G. KRAVIT, C. S. REGULA, and R. D. BERLIN

*Department of Physiology, University of Connecticut Health Center, School of Medicine, Farmington, Connecticut 06032*

**ABSTRACT** We studied the molecular form of tubulin in solution by ultrafiltration, nondenaturing electrophoresis, and chemical cross-linking. Our results are not consistent with the generally-held belief that tubulin in solution is a 110,000-mol-wt dimer. Rather, tubulin in solution consists of small oligomers; dimers are a minority species. The small proportion of dimers was readily apparent from ultrafiltration experiments. We first compared the filterability (defined as the ratio of protein concentration in filtrate to that applied to the filter) of phosphocellulose-purified tubulin (PC-tubulin) with aldolase (142,000 mol wt). Using an Amicon XM 300 filter, the filterability of PC-tubulin at room temperature and at a concentration of 0.5 mg/ml was only 0.12, whereas under the same conditions the filterability of aldolase was 0.60. We determined the average effective molecular weight of tubulin from its filterability on XM 300 filters calibrated with standard proteins. At room temperature, PC-tubulin at 0.5 mg/ml had an effective molecular weight of ~300,000. This molecular weight was significantly reduced at 10°C, indicating that oligomers dissociated at low temperatures.

Oligomers were also demonstrated by chemical cross-linking using glutaraldehyde, dimethyl suberimidate, and *bis*[2-(succinimidooxycarbonyloxy)ethyl] sulfone. In addition, PC-tubulin ran as a series of discrete bands in a nondenaturing PAGE system at alkaline pH. Quantitative examination of the mobilities of these bands and of standard proteins revealed that the bands represented a series of oligomeric forms. Similar electrophoretic patterns were observed in solutions of tubulin containing microtubule-associated proteins (MAPs) but with a shift to a greater proportion of higher oligomers. Nondenaturing PAGE at pH 8.3 showed that a shift towards higher oligomers also occurred in the absence of MAPs as the concentration of tubulin was increased. This concentration-dependence of oligomerization at room temperature was further demonstrated by ultrafiltration. When solutions of PC-tubulin at concentrations <0.25 mg/ml were ultrafiltered, filterability increased as concentration decreased. Quantitative studies of filterability following progressive dilution or concentration showed that this process was completely and rapidly reversible. A diffuse pattern of PC-tubulin on nondenaturing PAGE at pH 7 was observed and is consistent with a mixture of oligomers in rapid equilibrium.

We discuss the differences between our results and earlier results obtained by other methods with particular emphasis on the potential contribution of cold and hydrostatic pressure to the dissociation of oligomers. We also discuss the implications of oligomer formation for microtubule assembly.

Previous studies have indicated that tubulin dimers are the basic molecular building blocks of microtubules. This concept

is based in part on studies using ultracentrifugation (23) and column chromatography (17, 51), which indicate that solu-

tions of microtubule protein in vitro consist primarily of rings (containing microtubule-associated proteins [MAPs]<sup>1</sup> [35]) and tubulin dimers. Ultracentrifugation of purified tubulin at 4°C consistently shows a predominant 6S species (1, 6, 14, 30, 45, 56, 57). However, there is some evidence for oligomeric forms of tubulin that may be intermediates of assembly (9, 11, 19, 20, 34, 43).

We show here by three independent methods, ultrafiltration, nondenaturing PAGE, and chemical cross-linking, that at room temperature (20–23°C) only a small fraction of bovine tubulin in phosphate-glutamate buffer was present as simple dimer. Tubulin appeared to self-associate, even in the absence of MAPs, into a series of small oligomers. Oligomerization was rapid and concentration-dependent. The extent of oligomerization was reduced at low temperature and was freely reversible, indicating that oligomerization was not the result of denaturation.

## MATERIALS AND METHODS

GTP, Coomassie Brilliant Blue G250 and R250, Fast Green FCF, and dimethyl sulferimide (DMS) were obtained from Sigma Chemical Co. (St. Louis, MO). All proteins used as molecular weight markers were also purchased from Sigma Chemical Co., except for bovine IgG, which was obtained from Cappel Laboratories (West Chester, PA), and myosin, which was a gift from Drs. Susan Brawley and Peter Cooke (University of Connecticut Health Center). 5(4,6-Dichlorotriazin-2-yl) amino fluorescein dihydrochloride (DTAF) was purchased from Research Organics (Cleveland, OH). Sephadex G25 was a product of Pharmacia Fine Chemicals (Piscataway, NJ), while P11 phosphocellulose was supplied by Whatman Laboratory Products, Inc. (Clifton, NJ). Acrylamide was obtained from Bio-Rad Laboratories (Richmond, CA), *N,N'*-methylenebis-acrylamide from Eastman Laboratory and Specialty Chemicals (Rochester, NY), and sodium lauryl sulfate (SDS) was purchased from BDH (Carle Place, NY). Glutaraldehyde was purchased from Polysciences, Inc. (Warrington, PA), and bis-[2-(succinimido-oxycarbonyloxy)ethyl] sulfone (BSOCOES) was a product of Pierce (Rockford, IL). All salts and other chemicals were analytical grade.

**Protein:** Bovine brains were obtained locally and processed within an hour of slaughter. Three-times-cycled microtubule protein in 20 mM sodium phosphate, 100 mM sodium glutamate, pH 6.75 (PG buffer), was prepared according to the protocol of Margolis and Wilson (37), as modified by Regula et al. (46). Aliquots were stored at –80°C. No deterioration of the protein was detected after as long as 2 mo of storage. Labeling with DTAF was performed according to the procedure of Keith et al. (24) as follows: 5 mg/ml of assembled microtubule protein in 50 mM PIPES, 1.5 mM GTP, 1 mM EGTA, and 0.5 mM MgCl<sub>2</sub>, pH 6.75, was mixed with 0.05 vol of 5 mg/ml DTAF in dimethyl sulfoxide. The reaction was allowed to proceed at 30°C for 10 minutes after which it was terminated by the addition of a twofold molar excess of glutamine. The labeled microtubules were pelleted and taken through another cycle of assembly-disassembly in PG buffer. Any remaining free dye was removed by chromatography on Sephadex G25 columns. Phosphocellulose-purified tubulin (PC-tubulin) was prepared immediately before use by chromatographing three-times-cycled microtubule protein over columns of phosphocellulose equilibrated with ice-cold PG buffer at ratios of no more than 2 mg of protein per milliliter of phosphocellulose. Fractions were eluted with PG buffer and the protein content monitored with Coomassie Blue G250 (7). The tubulin elutes in the void volume.

**Ultrafiltration:** Amicon XM 300 filters (Danvers, MA) were extensively washed in water and assembled into either an Amicon Model 3 ultrafiltration cell or an Amicon MMC ultrafiltration manifold. The filters were then stirred for at least 30 min with PG buffer containing 0.1 mM EDTA (PGE), which, used to wash the filters and as the filtration medium, helped to reduce adsorption of proteins to the membrane. Presumably, competition between protein and glutamate amino groups reduced hydrogen bonding of protein to the carbonyl groups on the filter. Ultrafiltration of solutions of PC-tubulin,

often mixed with trace amounts of DTAF-labeled PC-tubulin, was performed with stirring under 10 psi of nitrogen. Filterability was expressed as the ratio of the concentration of protein in the filtrate to that applied to the filter. Only a small amount of filtrate (<10% of starting volume) was collected into tared tubes to minimize concentration changes during filtration. The tubes were reweighed to determine the amount of filtrate collected and the protein measured as described below. For the most accurate determinations of filtrate volumes, the collected volume was corrected for volume contributed by dead space in the apparatus. <sup>3</sup>H<sub>2</sub>O was added to the sample solution to a final concentration of 0.5 μCi/ml. From this specific activity and the total radioactivity in the filtrate, the actual sample volume filtered could be readily calculated.

To determine recovery, we stirred the retentate for at least 10 min, and an aliquot was taken for protein measurement. Typically ~88% of the applied protein was recovered in the combined filtrate and retentate. Variation in recovery was <5%. When appropriate, filterabilities obtained using different filters were normalized by comparing the filterabilities of a standard protein, bovine IgG, through these filters. All filterabilities were then multiplied by that factor that would bring the filterability of IgG to a fixed value. Filters were washed after standardization, first with buffer, then with 6 M urea overnight, and finally with distilled water, and reused for no more than one filtration, except where noted in the text.

We wish to emphasize that the cut-off of XM 300 filters at a molecular weight of 300,000 is nominal only. Moreover there appear to be difficulties in the reproducible manufacture of filters of large porosity. It is therefore imperative that each filter be characterized by its behavior toward proteins of known molecular size. For this purpose we have found that IgG serves as a convenient probe.

**PAGE:** Nondenaturing PAGE at pH 8.3 was performed using the Bryan system (8, 53) with a Laemmli (25) stacking gel, except that SDS was completely omitted. Nondenaturing PAGE at neutral pH was performed on 5% running gels buffered with 0.1 M NaPi, pH 7.0 with 3% stacking gels buffered with 0.02 M NaPi, pH 7.0. Electrophoresis buffer was 0.2 M NaPi, pH 7.0. SDS PAGE was performed using the procedure of Laemmli (25). Gels were stained with Coomassie Brilliant Blue R250 or quantitatively with Fast Green FCF (46). A Gilford 240 spectrophotometer (Oberlin, OH) equipped with linear transport was used to scan tube gels. A Hoeffer GS300 scanning densitometer (San Francisco, CA) was used to scan slab gels.

**Cross-linking:** The glutaraldehyde employed for cross-linking was an 8%, electron microscopy grade stock solution stored under nitrogen. 200 mM stock solutions of DMS in 0.2 M Tris, pH 9.2, and BSOCOES in dimethyl sulfoxide were prepared within 1 min of use. PC-Tubulin was prepared as already described, except that the columns were equilibrated and developed with 50 mM PIPES, pH 6.8. Incubations with glutaraldehyde or BSOCOES were performed in this buffer. For DMS cross-linking, the eluted protein was adjusted to 0.2 M Tris, pH 9.2, immediately before addition of cross-linker. DMS or BSOCOES was usually added to a final concentration of 2 mM, and the final concentration of glutaraldehyde was usually 0.15%. All reactions took place at room temperature. After appropriate incubation, reactions were stopped by the addition of a 100-fold molar excess of glycine or glutamine. Samples were immediately processed for SDS PAGE.

**Protein Assays:** Protein was determined using the method of Lowry et al. (31) or as modified by Bensadoun and Wettstein (3). When DTAF-labeled tubulin was used, its fluorescence ( $\lambda_{\text{excit}} = 480 \text{ nm}$ ;  $\lambda_{\text{em}} = 495 \text{ nm}$ ) was monitored using a Perkin-Elmer MDF44 fluorescence spectrophotometer (Perkin-Elmer Corp., Instrument Div., Norwalk, CT).

## RESULTS

### *Existence of Tubulin Oligomers: Ultrafiltration*

To determine the molecular dimensions of soluble tubulin with minimal perturbation, we filtered PC-tubulin at room temperature through an Amicon XM 300 filter whose nominal molecular weight cut-off was about 300,000. Remarkably, at a concentration of 0.5 mg/ml, tubulin had a filterability of less than 0.13 through a typical XM 300 membrane. Under the same conditions, aldolase (142,000 mol wt) had a filterability of about 0.60. This suggested that the molecular weight of tubulin in solution was significantly greater than 142,000, i.e., larger than a 110,000-mol-wt dimer.

To obtain a more precise estimate of the effective molecular weight of tubulin in solution we used two procedures. (a) An empirical relationship between filterability and molecular ra-

<sup>1</sup> *Abbreviations used in this paper:* BSA, bovine serum albumin; BSOCOES, bis[2-(succinimido-oxycarbonyloxy)ethyl] sulfone; DMS, dimethyl sulferimide; DTAF, 5(4,6-dichlorotriazin-2-yl) amino fluorescein dihydrochloride; PC-tubulin, phosphocellulose-purified tubulin; and PG buffer, 20 mM sodium phosphate, 100 mM sodium glutamate, pH 6.75.

dus was established using a series of proteins of known dimension. The molecular dimension of tubulin was then derived from its filterability by interpolation. (b) We employed the theory of restricted diffusion (26), which accounts for the hydrodynamic behavior during filtration of molecules whose dimensions approach pore size, to first calculate an effective filter pore size. Using this pore size and the measured tubulin filterability, the effective radius of tubulin could then be calculated (see Appendix).

The filterabilities of standard proteins and tubulin are given in Table I. It is seen at once that the filterability of tubulin is less than that of catalase (232,000 mol wt), but greater than that of myosin (468,000 mol wt). The filter pore size was calculated from the restricted diffusion theory (see Appendix) for each standard protein (Table I, last column). The close agreement of the calculated pore sizes indicated that the theory provided reasonable estimates of molecular dimensions over the range of protein molecular weights tested. Using the calculated pore size and the measured filterability of tubulin, we calculated that its effective average radius was 4.37 nm, corresponding to a molecular weight of 272,000. Fig. 1 is a plot of filterability vs. molecular weight. The continuous curve is calculated from theory using a pore radius of  $5.17 \pm 0.29$  nm (Table I); the individual experimental points are shown as open squares.

The value for the molecular weight of PC-tubulin approximates that of a pentamer. However, the measurement probably reflects the presence of mixed oligomeric forms whose average molecular weight is (fortuitously) near that of the pentamer. Indeed, other evidence presented below indicates the presence of multiple oligomeric forms. Nevertheless, the data allow one to set an upper limit to the fraction of tubulin present as dimer that is consistent with the filtration data. Assuming a spherical geometry, a 110,000-mol-wt dimer would have a radius of 3.18 nm (47). From this value and the theory (see Appendix), the predicted filterability of a solution containing only dimers is 0.23. The measured value of 0.03 indicates that not >13% (0.03/0.23) can be present as dimer.

During the course of our study, we encountered considerable variability in the filtration characteristics of individual filters. As indicated in Materials and Methods, testing of each filter was necessary. The normalization procedure employed based on the filterability of IgG appeared valid from the consistent data obtained for the standard proteins whose filterabilities were measured using different, separately-characterized filters. In addition, we succeeded in obtaining measurements of the filterabilities of a range of proteins and tubulin through the same filter. This method was taken to address the critical question of whether oligomers, like microtubules, are cold-sensitive. The measurements of filterability were made at room temperature and with the apparatus moved to a 4°C cold room. Under these conditions, the temperatures of the filtered solutions were actually ~10°C, probably due to the heat generated by the magnetic stirrer. Table II shows the filterabilities of the proteins through seven filters. We show the data for all filters so that their variability is apparent, as is the consistency of a given filter for the relative filterabilities of tubulin and a set of standard proteins. The mean filterabilities of IgG at 10°C and 22°C were identical. By contrast, the filterabilities of tubulin at 10°C were greater than at 22°C for all filters ( $P < 0.0005$ ). It is apparent from Table II that the mean filterabilities decreased monotonically with molecular weight. For clarity, we plotted in Fig. 2

TABLE I  
Filterability of Standard Proteins

Protein	Molecular Weight ( $\times 10^3$ )	Molecular radius (nm)	Normalized filterability*	Pore radius (nm)
Ovalbumin	40	2.33	0.620	5.16
BSA	67	2.69	0.421	5.10
Aldolase	142	3.47	0.241	5.64
IgG	160	3.60	0.073	4.84
Catalase	232	4.08	0.043	5.09
Myosin	468	5.40	0.000	*
PC-Tubulin	—	—	0.040	—
		Average radius		5.17
		Standard deviation		0.29

Approximately 0.5 mg/ml of IgG was filtered through each of seven filters. The exact starting and filtrate protein concentrations were determined, and the filterability of IgG was calculated for each filter. The filters were cleaned as described in Materials and Methods, and 0.5 mg/ml ovalbumin, BSA, aldolase, IgG, catalase, myosin, and tubulin at room temperature were filtered through them. The filterabilities of these proteins were determined as above and multiplied by the factor that would bring the filterability of IgG through that particular filter to 0.073. The radius of each protein was derived from its spherical equivalent (47), and the pore radius was calculated from Eq. 3 in the Appendix.

\* Ratio of the concentration of protein in the filtrate to that applied to the filter. To account for the variations between filters, filterabilities were normalized (see Materials and Methods) to an IgG filterability of 0.073.

\* Not calculable.

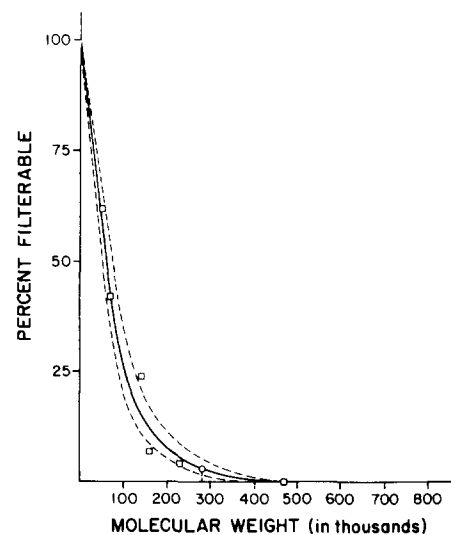


FIGURE 1 Normalized filterability at room temperature vs. molecular weight. The solid line represents a standard curve calculated using the pore radius given in Table I (5.17 nm) and derived using Eq. 3 in the Appendix. The dashed lines represent the curves obtained by using a pore radius one standard deviation unit (0.29 nm) greater or less than 5.17 nm. (□) Proteins of known molecular weights. (○) PC-Tubulin. The filterabilities were normalized as described in Materials and Methods to the least permeable filter. Approximately 0.5 mg/ml of the following proteins in PGE buffer were ultrafiltered: ovalbumin (42,000 mol wt), BSA (67,000 mol wt), aldolase (142,000 mol wt), IgG (160,000 mol wt), myosin (468,000 mol wt), and PC-tubulin. The ordinate, "Percent Filterable," corresponds to filterability  $\times 100$ .

the data from two filters (Nos. 2 and 5) for which the filterabilities of IgG were virtually identical. The effective molecular weight of PC-tubulin was 203,000 at 10°C and 297,000 at 22°C. Clearly, oligomers tended to dissociate at the lower temperature.

TABLE II  
Effect of Temperature on the Filterabilities of PC-Tubulin and IgG

Filter number	Filterability						
	BSA	Transferrin	IgG-10°C	IgG	PC-Tubulin-10°C	Catalase	PC-Tubulin
1	0.788	0.723	0.241	0.408	0.216	0.202	0.144
2	0.666	0.460	0.271	0.279	0.180	0.163	0.098
3	0.693	0.747	0.403	0.239	0.237	0.184	0.145
4	0.736	0.799	0.119	0.217	0.163	0.221	0.102
5	0.595	0.592	0.291	0.271	0.200	0.198	0.086
6	ND*	0.627	0.251	ND*	0.224	0.209	0.129
7	0.645	0.765	0.433	0.273	0.236	0.216	0.132
Average	0.687	0.673	0.287	0.281	0.208	0.199	0.119
Standard deviation	0.068	0.120	0.105	0.067	0.028	0.020	0.024

XM 300 filters were washed and assembled into an Amicon MMC manifold as described in Materials and Methods. The various proteins were dissolved and filtered in PGE buffer at a concentration of ~0.5 mg/ml. Except where noted, all filtrations were performed at room temperature. After each filtration, the filters were washed with 6 M urea as described in Materials and Methods.

\* ND, not determined.

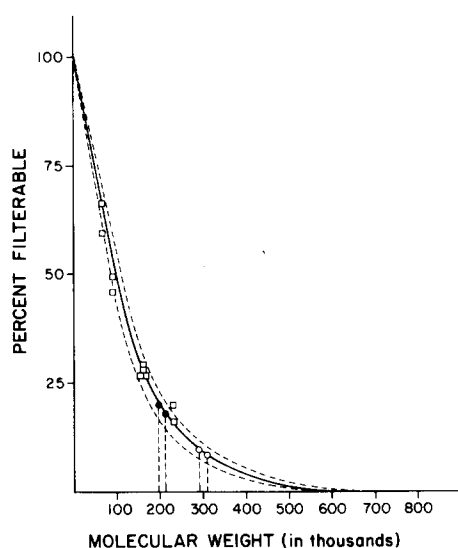


FIGURE 2 Filterabilities of PC-tubulin and standard proteins at room and low temperatures. The data for filters 2 and 5 from Table II are plotted as filterability vs. molecular weight. The solid line is the standard curve which was calculated as follows: the filterability of each standard protein was used to calculate a pore radius from Eq. 3 in the Appendix. These were averaged to give a mean pore radius of 5.97 nm, and this value was substituted into Eq. 3 to yield a standard curve. The dashed lines were calculated using this pore radius plus or minus one standard deviation unit (0.17 nm). (□) BSA, transferrin, IgG, and catalase. (○) PC-Tubulin at ~22°C. (●) PC-Tubulin at ~10°C. The ordinate, "Percent Filterable," corresponds to filterability  $\times$  100.

### Existence of Tubulin Oligomers: Electrophoresis under Nondenaturing Conditions

The existence of oligomers could be demonstrated independently by PAGE under nondenaturing conditions. On nondenaturing gels, PC-tubulin separated into at least 10 resolvable bands (Fig. 3, lanes e-j). There was also unresolved protein lying above the running and stacking gels. Under the same conditions, soybean trypsin inhibitor and bovine serum albumin (Fig. 3, lanes a-d) ran primarily as single bands. Unfractionated three-times-cycled microtubule protein showed the same multiple band pattern as the PC-tubulin

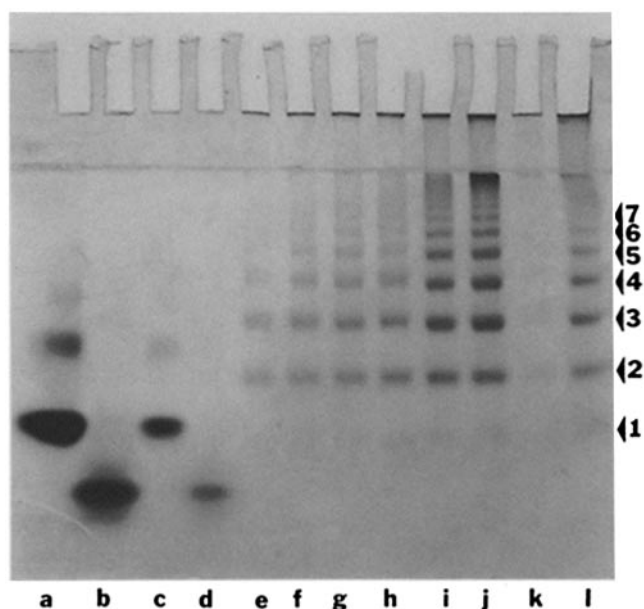


FIGURE 3 Nondenaturing PAGE of tubulin at pH 8.3. Various amounts of PC-tubulin, three-times-cycled microtubule protein, BSA, and soybean trypsin inhibitor were loaded in a 75  $\mu$ l volume onto the 3.5% stacking gel of a 6% nondenaturing slab gel. The gel was stained with Coomassie Brilliant Blue R250. (Lane a) 150  $\mu$ g BSA. (Lane b) 150  $\mu$ g soybean trypsin inhibitor. (Lane c) 20  $\mu$ g BSA. (Lane d) 20  $\mu$ g soybean trypsin inhibitor. (Lanes e-j) 20, 30, 40, 50, 100, and 150  $\mu$ g PC-tubulin, respectively. (Lane k) 20  $\mu$ g three-times-cycled microtubule protein. (Lane l) 150  $\mu$ g three-times-cycled microtubule protein.

(Fig. 3, lanes k and l).

It seemed likely that the tubulin bands corresponded to oligomers that were separated by both size and charge on native gels. Systematic examination of electrophoresis in gels of different porosity showed that the apparent molecular weights of the bands corresponded to multiples of tubulin dimers. When nondenaturing PAGE is performed at several acrylamide concentrations, and the log of the mobility ( $R_f$ ) of a protein of known molecular weight at each concentration is plotted against the acrylamide concentration, a straight line should result in which the slope is proportional to the retardation coefficient ( $K_R$ ) (47). Fig. 4A shows such a plot for

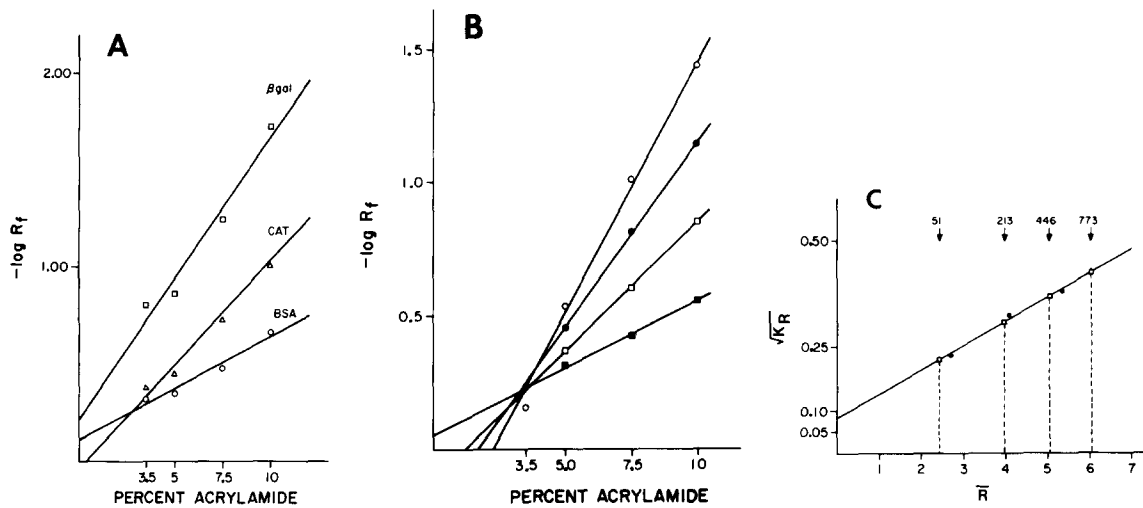


FIGURE 4 Mobilities of standard proteins and tubulin bands on nondenaturing PAGE at pH 8.3. (A) Standard proteins. 3.5%, 5%, 7.5%, and 10% nondenaturing tube gels with 3% stacking gels were run as described in Materials and Methods. The gels were stained with Coomassie Brilliant Blue R250 and the positions of the dye fronts and bands determined by scanning densitometry at 525 nm.  $R_f$  is the relative mobility. The retardation coefficient,  $K_R$ , was determined as the slope of a line calculated by linear regression. (□)  $\beta$ -Galactosidase (520,000 mol wt). ( $\Delta$ ) Catalase (232,000 mol wt). (○) BSA (67,000 mol wt). (B) The four fastest migrating tubulin bands.  $K_R$  was determined in the same manner as described in A. (■) Fastest moving band. (□) Second fastest moving band. (●) Third fastest band. (○) Fourth fastest band. (C) Determination of radii of tubulin species. The radii of  $\beta$ -galactosidase, catalase, and BSA are given by Rodbard and Chrambach (47) and are calculated assuming a spherical shape and a molar specific volume of  $0.74 \text{ cm}^3 \text{ g}^{-1} \text{ mol}^{-1}$ . The square root of  $K_R$  (●) calculated from the data of A for each protein was plotted against its radius, and a standard curve was calculated using linear regression. The radii for the tubulin bands (□) were derived from measured  $K_R$ 's and the standard curve. The molecular weights were calculated assuming a spherical shape and a specific volume of  $0.736 \text{ cm}^3 \text{ g}^{-1} \text{ mol}^{-1}$  (23). As shown at the arrows, these molecular weights are 51,000, 213,000, 446,000 and 773,000.

three molecular weight standards, and Fig. 4B shows the equivalent plots for the four fastest migrating tubulin bands. A plot of the square root of  $K_R$  against molecular radius for the series of proteins of known dimensions yields a standard curve (47) from which the dimensions of the tubulin oligomers can be estimated. Fig. 4C shows this standard curve and the values obtained from it for the radii of the four fastest migrating bands. These molecular dimensions are consistent with the molecular weights of a linear series of oligomers, the diffuse, fastest band being a mixture of  $\alpha$ - and  $\beta$ -subunits, (mean molecular weight 51,000) followed by tetramer, hexamer, and octamer (213,000, 446,000, and 773,000 mol wt, respectively).

#### Existence of Tubulin Oligomers: Chemical Cross-linking of Tubulin Solutions

Chemical cross-linking reagents are used widely to demonstrate the proximity of protein subunits. If tubulin in solution exists as oligomers, it should be possible to show a high degree of intermolecular cross-linking under conditions in which cross-linking of monomers of other proteins does not occur. Fig. 5 shows SDS PAGE of PC-tubulin that had been incubated at room temperature for various intervals with glutaraldehyde. The positions of several bands clearly indicated the presence of higher oligomers. There was a progressive increase with time in the amount of tubulin that failed to enter both the running and even the stacking gels, and, concomitantly, there was a progressive loss in the  $\alpha$ - and  $\beta$ -tubulin monomer bands. In addition, several higher molecular weight bands were also seen to increase with incubation. These included bands at roughly 165,000 and 220,000 and others at still higher molecular weights. Interestingly, there

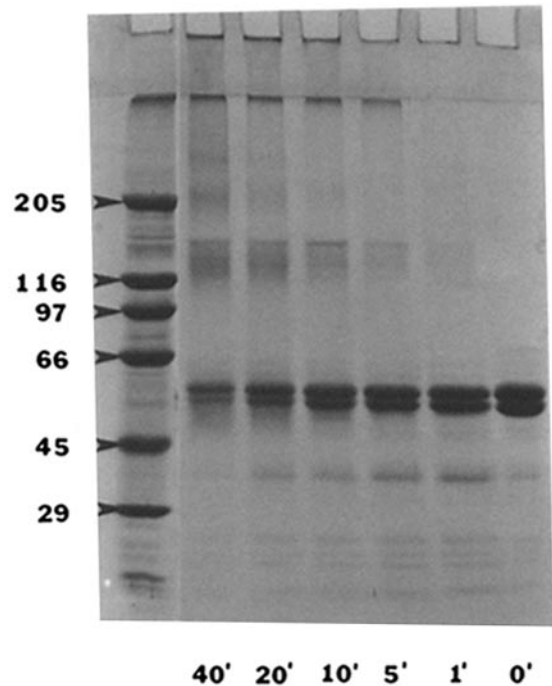


FIGURE 5 SDS PAGE of glutaraldehyde cross-linked tubulin as a function of time of incubation. 1-mg/ml aliquots of PC-tubulin were cross-linked with 0.15% glutaraldehyde at room temperature for various lengths of time. The reactions were stopped with a 20-fold molar excess of glycylamide, and 40  $\mu\text{g}$  of each was loaded onto the 3.5% stack of a 5–12% linear gradient gel. The gel was stained with Coomassie Blue R250. The time of cross-linking of each sample is shown beneath the corresponding lane. Standards are shown in the far left lane.

was no prominent band corresponding to tubulin dimer, which suggests that it was a transient intermediate in the cross-linking process. Similar patterns of chemically cross-linked tubulin were seen following incubations with BSO-COES (59) at pH 6.9 and DMS at pH 9.2 (Fig. 6). The glutaraldehyde-induced patterns are shown in Fig. 6, lanes *b* and *e*, for 0.4 mg and 2.0 mg/ml PC-tubulin, respectively. Fig. 6, lanes *c* and *f*, are the corresponding DMS, and Fig. 6, lanes *d* and *g*, the corresponding BSO-COES patterns. Bands of molecular weights of 110,000 and 165,000 in Fig. 6, lane *g*, and 220,000 and 275,000 in Fig. 6, lane *f*, are indicated by asterisks. Careful inspection of the 110,000 region in unphotographed gels of BSO-COES-cross-linked material showed a distinct triplet, no member of which was dominant. A similar triplet was investigated by Ludueña et al. (32) and shown to be consistent with  $\alpha$ - $\alpha$ -,  $\alpha$ - $\beta$ -, and  $\beta$ - $\beta$ -dimers. This suggests either that in addition to the  $\alpha$ - $\beta$ -heterodimer,  $\alpha$ - $\alpha$ - and  $\beta$ - $\beta$ -homodimers are present in solution, or, more likely, that the bands represent portions of higher oligomers that were incompletely cross-linked. At the same concentrations of protein and cross-linking reagents, non-oligomeric proteins such as ovalbumin were not cross-linked (data not shown).

Further evidence for higher tubulin oligomers was found in examination of cross-linking as a function of total protein concentration. It is anticipated that cross-linking of true oli-

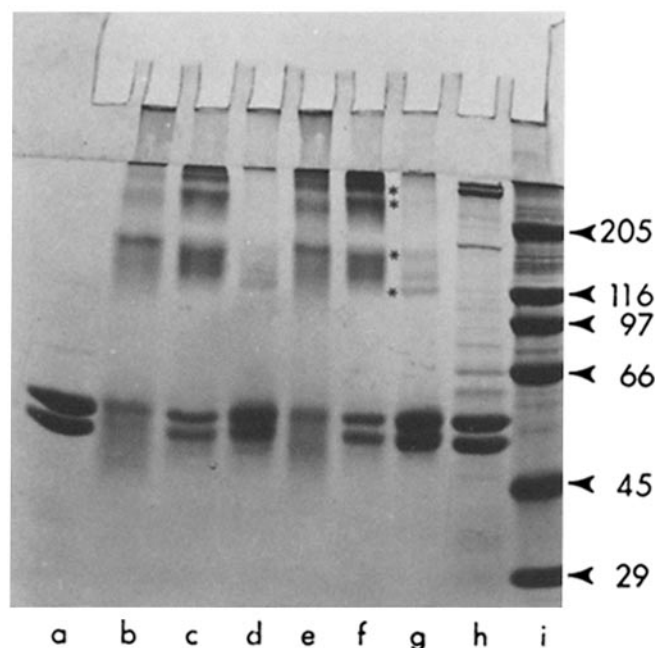


FIGURE 6 SDS PAGE of PC-tubulin cross-linked with three different reagents. PC-Tubulin, at either 0.4 or 2 mg/ml, was incubated with 0.15% glutaraldehyde, 2 mM DMS, or 2 mM BSO-COES for 20 min at room temperature. The reaction was stopped with glycylamide, and 40  $\mu$ g of protein in a final volume of 100  $\mu$ l was loaded onto the 3.5% stack of a 7.5% slab gel. The gel was stained with Coomassie Blue R250. (Lane a) PC-Tubulin, untreated. (Lane b) 0.4 mg/ml PC-tubulin, 0.15% glutaraldehyde. (Lane c) 0.4 mg/ml PC-tubulin, 2 mM DMS. (Lane d) 0.4 mg/ml PC-tubulin, 2 mM BSO-COES. (Lane e) 2 mg/ml PC-tubulin, 0.15% glutaraldehyde. (Lane f) 2 mg/ml PC-tubulin, 2 mM DMS. (Lane g) 2 mg/ml PC-tubulin, 2 mM BSO-COES. (Lane h) three-times-cycled microtubule protein. (Lane i) molecular weight standards. The asterisks indicate the positions of the 110,000- and 165,000-mol-wt cross-linked species (lane g) and of the 220,000- and 275,000-mol-wt cross-linked species (lane f).

gomers will be relatively unaffected by total protein concentration except at extreme dilution, whereas random collisional events are proportional to the square of the protein concentration (10). Fig. 7 shows that the degree of cross-linking was relatively unaffected over a fivefold range of concentration.

#### Effect of Concentration on the Degree of Oligomerization

Two different lines of evidence based on ultrafiltration and nondenaturing PAGE showed that the extent of tubulin oligomerization at room temperature was concentration-dependent. When solutions of tubulin at various concentrations were ultrafiltered, their filterability was essentially constant  $>0.25$  mg/ml. However, at concentrations  $<0.25$  mg/ml, the filterability of PC-tubulin increased progressively with decreasing concentration. Thus, oligomers clearly dissociated at low concentration. Fig. 8 shows a composite of two experiments in which the filterability of PC-tubulin is plotted vs. the concentration of tubulin in the applied sample. The results fit a biphasic curve that is semilogarithmic at concentrations below  $\sim 0.25$  mg/ml and almost flat above 0.25 mg/ml.

We have ruled out two alternative explanations for the concentration dependence of filtration: clogging of filter pores at high protein concentrations, and a phenomenon known as concentration-polarization, in which filter-rejected solute builds up near the membrane in sufficient concentration to form a secondary filter (5). Both clogging and concentration-

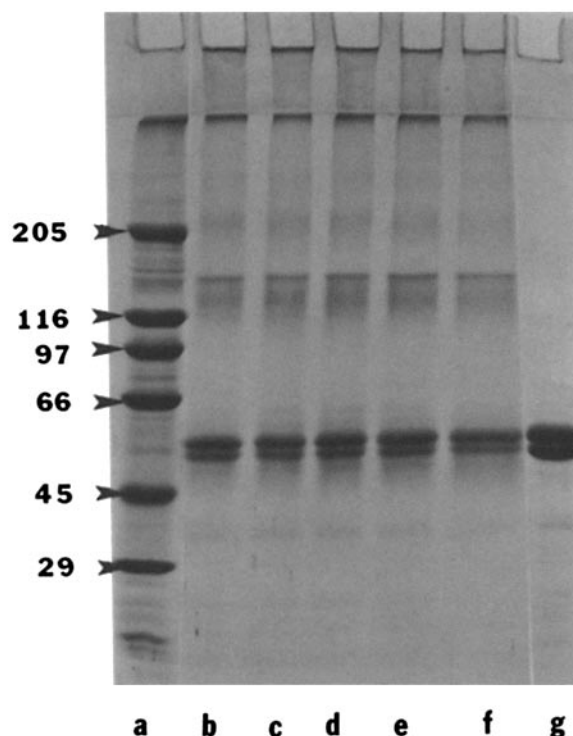


FIGURE 7 SDS PAGE of tubulin cross-linked with glutaraldehyde at different protein concentrations. 0.15% Glutaraldehyde was incubated with different concentrations of PC-tubulin at room temperature. After 20 min, the reactions were stopped with a 20-fold molar excess of glycylamide, and 40  $\mu$ g of each were loaded onto a 5–12% linear gradient gel with a 3.5% stack. (Lane a) Molecular weight standards. (Lane b) 0.4 mg/ml. (Lane c) 0.8 mg/ml. (Lane d) 1.2 mg/ml. (Lane e) 1.6 mg/ml. (Lane f) 2.0 mg/ml. (Lane g) Untreated PC-tubulin.

polarization should occur in solutions of proteins other than tubulin, such as IgG. In addition, when different proteins are mixed each constituent should be affected by clogging or concentration-polarization. We showed first that the filterability of IgG was independent of protein concentration over the same range as that used for tubulin. Thus the filterabilities of IgG at 0.1, 0.2, 0.3, and 0.5 mg/ml were not different, and, for the particular XM 300 filter employed, averaged 0.473 with a standard deviation of only 0.045 over all of the concentrations. An even more stringent control is summarized in Table III. In these experiments (which used the identical filter) mixtures of tubulin and transferrin were filtered. Clearly the presence of 0.5 mg/ml transferrin did not modify the concentration dependence of tubulin filterability. Moreover,

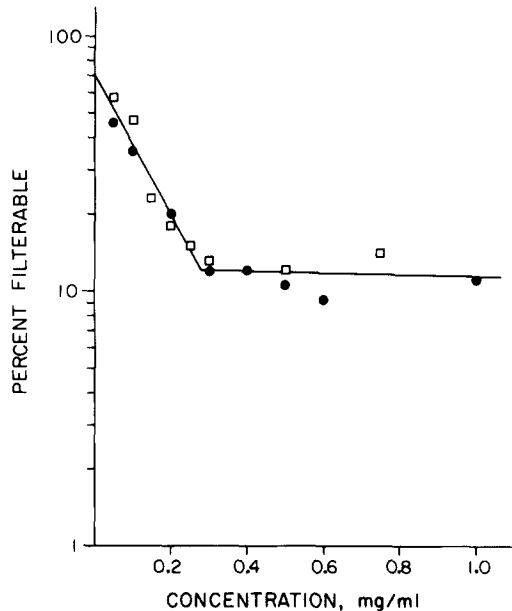


FIGURE 8 Effect of PC-tubulin concentration on its filterability. PC-Tubulin was prepared from three-times-cycled microtubule protein that had been mixed with a small amount of DTAF-labeled microtubule protein, and then diluted with PGE buffer to final concentrations of 0.05 to 1 mg/ml. The solutions were filtered through XM 300 membranes as described in Materials and Methods and protein concentrations monitored both by Lowry (not shown) and by fluorescence. The different symbols represent two separate experiments, and the lines were calculated by a linear regression analysis. The ordinate, "Percent Filterable," corresponds to filterability  $\times$  100.

TABLE III  
Effect of Transferrin on Tubulin Filterability

Filtration	Concentration of transferrin applied to filter (mg/ml)	Concentration of PC-tubulin applied to filter (mg/ml)	Transferrin filterability	Tubulin filterability
1	0.5	0.5	0.690	0.187
2	0.5	0.1	0.636	0.518
3	0.1	0.1	0.693	0.614

Transferrin and PC-tubulin were dissolved to the given concentrations in PGE buffer, and the mixture was filtered through an XM 300 filter as described in Materials and Methods. The filterability of IgG through this membrane was 0.473. Known volumes of filtrates and starting solutions were electrophoresed on 7% Laemmli gels and stained quantitatively with Fast Green FCF. The stained gels were scanned and the areas under the tubulin and transferrin peaks were quantified and used to calculate filterabilities.

the filterability of transferrin was unaffected by its concentration. The concentration dependence of tubulin oligomerization was therefore not an artifact of the filtration process.

A dependence of oligomer formation on concentration could also be demonstrated on nondenaturing polyacrylamide gels. Fig. 3 shows a nondenaturing slab gel of different amounts of tubulin loaded in identical volumes. The distribution of tubulin into its various bands changed with the concentration, shifting to a higher proportion of slower moving bands with increasing concentration. The quantitation of the concentration effect is shown in Fig. 9. As the concentration of tubulin increased, so did the proportion of the higher order oligomers.

### Reversible Formation of Oligomers at Room Temperature

To examine the possibility that oligomerization was the result of tubulin denaturation and aggregation, we tested its reversibility. A solution of PC-tubulin was diluted, stirred for 10 min, filtered, diluted to a new concentration, and so on for three cycles. The results are shown in Table IV. The filterability at each concentration was in close agreement with previous determinations in which the tubulin was only filtered once.

Conversely, a dilute solution of PC-tubulin was filtered progressively (Table V). As it became concentrated, periodic samples of filtrate and retentate were taken. After each filtration step, the solution was stirred for 2 min. Again, the filterability at each concentration was in good agreement with previous determinations in which the tubulin was only filtered once. Thus, there was no decay of the ability of the tubulin to dissociate or reassociate during this experiment. Oligomerization was therefore freely reversible and was not a conse-

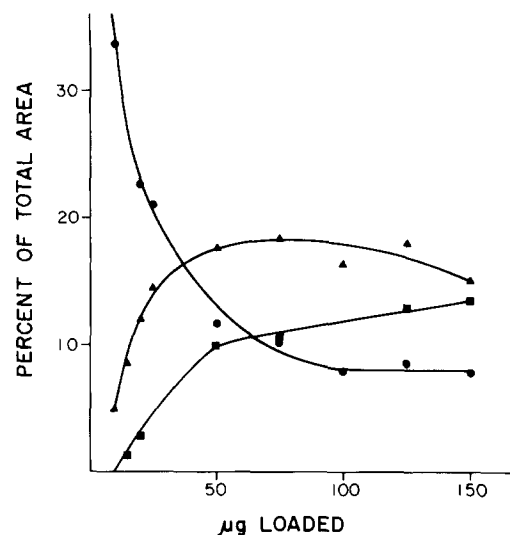


FIGURE 9 Proportion of PC-tubulin in different bands on nondenaturing PAGE as a function of the concentration applied. 6% nondenaturing tube gels were run as described in Materials and Methods using various amounts of PC-tubulin in a constant loading volume of 50  $\mu$ l. The gels were quantitatively stained with Fast Green FCF, scanned at 625 nm, and the areas under the peaks determined using a sonic digitizer (Graf Pen [Science Accessories Corp., Southport, CT]). The percentage of total resolvable area in a given peak is plotted against micrograms loaded for three representative bands. (●), 2nd fastest migrating band. (▲), 5th fastest migrating band. (■), 7th fastest migrating band.

TABLE IV  
Filterability of PC-Tubulin during Progressive Dilution

Filtration	Concentration of PC-tubulin applied to filter (mg/ml)	Filterability predicted from Fig. 8	Actual filterability
1	0.500	0.120	0.084
2	0.235	0.155	0.157
3	0.126	0.317	0.255

PC-Tubulin was diluted to 0.5 mg/ml and a small amount was filtered at room temperature through an Amicon XM 300 membrane at 10 psi of nitrogen. The retentate was stirred for 10 min and PGE buffer was added. A sample of the diluted retentate was taken and the solution refiltered. The retentate was stirred, diluted, sampled, and refiltered for another two cycles. The filterability for each cycle was calculated.

TABLE V  
Filterability of PC-Tubulin with Progressive Concentration

Filtration	Concentration of PC-tubulin applied to filter (mg/ml)	Filterability predicted from Fig. 8	Actual filterability
1	0.085	0.415	0.400
2	0.107	0.359	0.290
3	0.113	0.345	0.301
4	0.123	0.323	0.293
5	0.131	0.307	0.313
6	0.146	0.278	0.267
7	0.161	0.252	0.236
8	0.193	0.204	0.187
9	0.245	0.145	0.188
10	0.405	0.120	0.133

PC-Tubulin was diluted to 0.085 mg/ml and filtered through an Amicon XM 300 membrane at room temperature and 10 psi of nitrogen. The retentate was stirred for 2 min, sampled, and refiltered. This was repeated through a total of 10 cycles.

quence of tubulin denaturation.

Since some of the solutions in the stepwise filtrations were allowed only 2 min to reequilibrate, the approach to equilibrium must be fairly rapid. The rapid equilibrium makes it impossible to discern the role of oligomers in assembly using separation techniques. After an ultrafiltration, for example, re-equilibration occurred so that both filtrate and retentate were able to polymerize onto axonemal seeds with a critical concentration similar to that of unfractionated PC-tubulin (unpublished observations).

A rapid equilibrium seems to be inconsistent with the results of the nondenaturing PAGE experiments shown in Figs. 3 and 9, since Gilbert (21) has shown that species in rapid equilibrium do not form discrete bands, but rather "equilibrium smears." However, our gels were run at alkaline pH, a condition which is known to inactivate tubulin for assembly (46). When gels were run at neutral pH, the expected "smear" was obtained. Fig. 10 shows nondenaturing PAGE of PC-tubulin and BSA run at pH 7. BSA (Fig. 10, lane a) exhibits discrete bands, but PC-tubulin (Fig. 10, b) shows a smear from the interface of the stacking and running gels to just below the major BSA band, with the most intense Coomassie Blue staining located towards the top of the gel. The most straightforward interpretation of these results is that at pH 7, PC-tubulin is an equilibrium mixture of oligomers ranging in size from some dissociated monomer to very large assemblages, with the majority of the tubulin being in high-

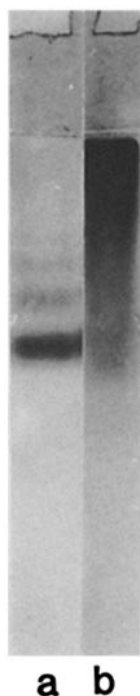


FIGURE 10 Nondenaturing PAGE of PC-tubulin and BSA at neutral pH. PC-Tubulin and BSA were run on nondenaturing gels at pH 7 as described in Materials and Methods. (Lane a) 20  $\mu$ g BSA. (Lane b) 40  $\mu$ g PC-tubulin.

molecular weight forms. At high pH, the approach to equilibrium is presumably either very much slower or abolished.

## DISCUSSION

We originally applied ultrafiltration to solutions of tubulin with the objective of separating free from membrane-bound tubulin. The small filterability of tubulin solutions actually observed and explored in this study appears to contradict the generally accepted view, based on numerous analyses of its sedimentation (e.g., 6, 14, 30, 45, 56, 57) and chromatographic (e.g., 14, 51, 56) behavior that tubulin in solution is predominantly dimeric. Yet it was clear from the outset that there are characteristics of ultrafiltration such as low hydrostatic pressure that set it apart from other techniques. These characteristics and the conditions of our experiments make it possible to reconcile our observations with the extensive literature in which the molecular dimensions of tubulin have been determined by ultracentrifugation and column chromatography.

First, the majority of ultracentrifugations and chromatography has been performed at 4°C. We were not able for technical reasons to perform the ultrafiltration at temperatures as low as 4°C, but even at 10°C, the cold-induced dissociation of oligomers was clear. In view of the well-known cold-induced disassembly of microtubules, this should not be surprising.

Second, it is also known that microtubules are pressure-sensitive (48), and it has been shown that the 30S ring oligomers found in solutions of tubulin with MAPs as well as microtubules themselves are disassembled by hydrostatic pressures during prolonged ultracentrifugation (35, 36). Similarly, it is possible that the oligomeric structures of PC-tubulin we have described are dissociated by high hydrostatic pressure. Indeed, we have shown in preliminary experiments in which ultracentrifugation is achieved at low hydrostatic pressures that tubulin at room temperature sediments at rates consistent with higher oligomers and not as a dimer.



The conditions used for most chromatographic studies may also lead to dissociation of oligomers: (a) most columns are developed in the cold, a condition that favors dissociation of oligomers; (b) the protein is subject to dilution, which we showed favors dissociation; and (c) studies of whole microtubule protein (tubulin and MAPs) are designed to separate MAPs or MAP-tubulin oligomers from free tubulin and not to define the molecular weight of free tubulin. For example, Sloboda et al. (51) were able to separate MAP-containing tubulin oligomers from free tubulin on Bio-Gel A-1.5 m. The column was run at 4°C and the position of the free tubulin in the elution profile would be easily compatible with oligomers of the size identified in our study.

Finally, we have consistently used bovine brain tubulin prepared in PG buffer without glycerol. While it is possible that our tubulin behaves differently than other mammalian brain tubulins prepared in PIPES or other buffers, our tubulin appears to behave like other tubulins in all major respects (see, for example, reference 46). Consequently, we do not believe that we are looking at a phenomenon peculiar to our preparation of bovine brain tubulin.

Our conclusion, based both on our results and on the literature, is that oligomers may be formed by cold- and pressure-sensitive bonds similar to those of the microtubule itself. Because of these properties, the existence of oligomers may have been obscured by temperatures and other factors operative in ultracentrifugation and gel chromatographic procedures, but which do not affect ultrafiltration.

Chemical cross-linking afforded another means of probing for the presence of oligomers without physical perturbation. Cross-linking at neutral and alkaline pH yields stable high molecular weight complexes of tubulin under conditions in which other protein monomers are not significantly cross-linked. The time course of tubulin cross-linking shows that high molecular weight species are detected early at low concentrations of reagent and are not changed over a range of protein concentration that would affect diffusion-dependent cross-linking of inherently non-oligomeric species.

The presence of oligomeric tubulin is consistent with protein patterns obtained in the absence of denaturing detergent by PAGE, a technique that has been used previously to study oligomerization processes. Insulin, for example, has been studied by nondenaturing PAGE (22), as has spectrin (38, 39). However, both spectrin and insulin can be induced to form large oligomers only at protein concentrations 10–100-fold higher than those employed in this study. When PC-tubulin is electrophoresed on nondenaturing gels at pH 7, a smear is present, as expected for molecules in a rapidly equilibrating interaction (21). The pH 8.3 gel pattern reveals a linear series of oligomers: monomer, tetramer, hexamer, etc. The relative proportions of these species are shown to be concentration-dependent. It cannot be asserted, of course, that these proportions exist in solution. It is known that PAGE tends to concentrate proteins in the stacking gel, so that indeterminate local concentrations of tubulin are actually present. The absence of dimers and the presence of monomers on these gels is puzzling. Indeed, a band corresponding to dimer on nondenaturing gels has been observed by Lee et al. (30); however, in this earlier study the tubulin was prepared by repeated salt fractionations including precipitation by  $MgCl_2$ , which can modify the circular dichroism (43) and the electrophoretic behavior of tubulin (unpublished observations). We suggest that on our gels dimers are dissociated

during electrophoresis to form the diffuse leading band. Such a dissociation could come about as follows:  $\alpha$ - and  $\beta$ -tubulins have different isoelectric points and probably carry different net charges; the electrical force acting upon them (product of voltage and charge) will thus be different as will their mobilities unless the intermolecular attractive force is sufficiently great. Conversely, the absence of dissociation of the higher oligomers in the gel suggests that when multiple subunits are present, cooperative intermolecular forces between them exceed the dissociative electrical field or that irreversible denaturation of the oligomeric species has occurred during electrophoresis.

It should be noted that oligomers analyzed by ultrafiltration were not produced by aggregation of denatured species. The most critical experimental evidence against denaturation was the series of filtrations with progressive concentration or dilution of the same tubulin solution. These showed clearly that oligomerization was reversible. In addition, the tubulin employed in all of our experiments was prepared and held in the cold until used, within an hour of its column purification. Finally, both filtrate and retentate polymerized onto axonemal seeds at approximately the critical concentration of unfiltered tubulin (unpublished observations).

We would emphasize that, whereas a distinct oligomeric species of tubulin has been detected before, this high molecular weight (30S) ring structure (or related 18 or 20S oligomers) (35, 36) contains MAPs. Although we do show protein bands consistent with oligomers on nondenaturing gels of whole microtubule protein (Fig. 3) our studies have focused primarily on the behavior of PC-purified tubulin, which contains <5% of other proteins as determined by SDS PAGE.

What is the relationship of oligomers to assembly? For some time, microtubule assembly has been viewed from the perspective of the assembly of tobacco mosaic virus. Indeed, tobacco mosaic virus and microtubule assembly have many parallels. Both are hydrophobic, entropy-driven processes (27–29). Both proteins form double layer discs, as well as related polymorphic forms (15, 16, 35, 49). In both cases discs appear to be used early in the assembly process (40, 44, 52). TMV elongation has been thought to proceed by addition of single subunits in a nucleation-condensation mechanism (40). The kinetics of this model have been worked out in detail (42). Since most studies of microtubule protein have not demonstrated oligomers and have shown the first order kinetics predicted for a nucleation-condensation mechanism (4), it has been suggested that microtubules like tobacco mosaic virus are elongated by the addition of single (dimeric) subunits. In fact, elongation by addition of oligomers may also be consistent with a nucleation-condensation mechanism.

The advantages of direct assembly from MAP-containing oligomers have been suggested by Weisenberg (58). In his scheme, oligomers are assembled preferentially, and the stability of oligomer association with a microtubule end depends on the extent of intersubunit bonding between the oligomer and the assembled microtubule subunits, which in turn depends on the area of surface contact between them. When an oligomer is fitted into a growing end, a large number of bonds can be formed resulting in high stability. We believe that this argument applies equally well to oligomers without MAPs. Further, the critical concentration for assembly may be the concentration at which oligomers of a preferred size are sufficiently abundant. Indeed, many other aspects of micro-

tubule assembly may need to be re-examined in view of the predominance of oligomers in solution.

The possibility of assembly of microtubules from oligomers suggests that regulation of oligomerization may be another level of control of microtubule polymerization in vivo. Cells may regulate microtubule formation on nucleation sites by controlling oligomer formation by mechanisms unknown, perhaps using a molecule analogous to the various actin-binding proteins (13, 33, 50, 54, 55). This may help explain how some cells, such as neuroblastoma, maintain concentrations of unpolymerized tubulin higher than the critical concentration (41).

It has also been hypothesized that the level of transcription of the tubulin gene(s) is controlled by the level of free tubulin dimer (2, 12). Our findings raise the question of whether a unique oligomeric species of tubulin (which would increase with total free concentration and may itself be regulated) is an essential element in the feed-back control.

## APPENDIX

The behavior of molecules filtered through pores of similar size can be described by the theory of restricted diffusion. As formulated by Landis and Pappenheimer (26), this states that

$$C_F/C_R = \left(1 + \frac{D_s A_w}{Q_f \Delta X}\right) / \left\{ \frac{D_s A_w}{Q_f \Delta X} + \frac{[2(1 - a_w/r)^2 - (1 - a_w/r)^4] \cdot [1 - 2.10(a_w/r) + 2.09(a_w/r)^3 - 0.95(a_w/r)^5]}{[2(1 - a_s/r)^2 - (1 - a_s/r)^4] \cdot [1 - 2.10(a_s/r) + 2.09(a_s/r)^3 - 0.95(a_s/r)^5]} \right\} \quad (1)$$

where  $C_F$  is the concentration of solute in filtrate;  $C_R$  the concentration of solute in retentate;  $D_s$  the diffusion constant of solute;  $A_w$  the area of pore available to water;  $Q_f$  the quantity filtered per unit time;  $a_w$  the radius of water molecule;  $a_s$  the radius of solute;  $\Delta X$  the thickness of membrane;  $r$  the radius of pore. For the XM 300, the ratio  $a_w/r$  approaches 0. This also means that  $A_w$  is approximately equal to  $\pi r^2$ . Finally, substituting  $D_s = RT/6\eta a_s N$ , where  $R$  is the gas constant,  $T$  the absolute temperature,  $\eta$  the viscosity of solvent, and  $N$  the Avogadro's number, simplifies Eq. 1 to the following:

$$C_F/C_R = \left(1 + \frac{r^2 RT}{a_s 6 N Q_f \Delta X}\right) / \left\{ \frac{r^2 RT \pi}{a_s 6 \eta N Q_f \Delta X} + \frac{1}{[2(1 - a_s/r)^2 - (1 - a_s/r)^4] \cdot [1 - 2.10(a_s/r) + 2.09(a_s/r)^3 - 0.95(a_s/r)^5]} \right\} \quad (2)$$

$RT\pi/6\eta N Q_f \Delta X$  consists of known quantities and is equal to  $1.08 \text{ nm}^{-1}$  for the XM 300 at 10-psi filtration pressure. In addition, filtration is performed under conditions in which  $C_R$  is approximately equal to the starting concentration. As a result,

$$\text{filterability} = (1 + 1.08(r^2/a_s) \text{nm}^{-1}) / \left\{ 1.08(r^2/a_s) \text{nm}^{-1} + \frac{1}{[2(1 - a_s/r)^2 - (1 - a_s/r)^4] \cdot [1 - 2.10(a_s/r) + 2.09(a_s/r)^3 - 0.95(a_s/r)^5]} \right\} \quad (3)$$

By filtering a protein of known molecular radius (calculated from a spherical equivalent of the molecular weight) and measuring the filterability, one is left with an equation in only one unknown,  $r$ .

The equation cannot be solved analytically, but  $r$  can be approximated to any desired accuracy by iteration. The final test of the theory is shown in Table I. IgG was filtered through each of five filters. Then five other protein standards were filtered through the same filters. Each filterability was multiplied by a correction factor derived from the IgG filterability for that filter in order to eliminate the differences among individual filters. Since Eq. 3 cannot be solved for  $r$  if the filterability is greater than 1, the data were normalized to the filter with the smallest IgG filterability, in order to have all five corrected filterabilities

less than 1.

The calculated pore sizes derived from the filterabilities of five proteins are in remarkable agreement: the mean pore size of the least permeable filter was 5.17 nm with a standard deviation of only 0.29 nm. When all of the standardizing proteins are filtered through a single filter, as in filters 2 or 5 of Table II, the standard deviation drops to <0.17 nm. These two filters have a more usual IgG filterability, about 0.28, corresponding to a pore radius of 6.0 nm.

The pore radius of an XM 300 has been measured to be 12.5 nm using the electron microscope (18). The agreement between the electron microscope and hydrodynamic determinations is quite good considering the variation among individual membranes and the fact that Eq. 1 assumes a cylindrical pore while the actual pores are tortuous. Once a value for  $r$  is known, one can solve the restricted diffusion equation either directly for filterability given the radius of the solute, or by iteration for solute radius, given filterability.

This work was supported by National Institutes of Health grant CA15544.

Received for publication 8 February 1983, and in revised form 25 January 1984.

*Note Added in Proof:* It should be emphasized that, to use ultrafiltration for the determination of molecular weight, it is necessary to choose carefully conditions that minimize concentration-polarization: low pressure (10 psi), low protein concentration (<1 mg/ml), and collection of small volumes of ultrafiltrate (<500  $\mu$ l). In any event, significant concentration-polarization must be ruled out by control experiments in which filterability of standard proteins and mixtures—“Effect of Concentration of Degree of Oligomerization.” Not surprisingly, as shown by Siezen (Siezen, R. J., 1984, *Biophys. Chem.*, 19:49–55), when conditions are chosen that promote concentration-polarization, ultrafiltration cannot be used to determine molecular weight.

## REFERENCES

1. Bayley, P. M., P. A. Charlwood, D. C. Clark, and S. R. Martin. 1982. Oligomeric species in glycerol-cycled bovine brain microtubule protein. Analytical ultracentrifuge characterization. *Eur. J. Biochem.* 121:579–585.
2. Ben-Ze'ev, A., S. R. Farmer, and S. Penman. 1979. Mechanisms of regulating tubulin synthesis in cultured mammalian cells. *Cell* 7:319–325.
3. Bensadoun, A., and D. Wettstein. 1976. Assay of proteins in the presence of interfering materials. *Anal. Biochem.* 70:241–250.
4. Bergen, L. G., and G. G. Borisy. 1980. Head-to-tail polymerization of microtubules in vitro. Electron microscope analysis of seeded assembly. *J. Cell Biol.* 84:141–150.
5. Blatt, W. F., A. David, A. S. Michaels, and L. Nelsen. 1970. Solute polarization and cake formation in membrane ultrafiltration: causes, consequences, and control techniques. In *Membrane Science and Technology*. J. E. Flinn, editor. Plenum Press, London. 47–97.
6. Borisy, G. G., J. B. Olmstead, and R. A. Klugman. 1972. In vitro aggregation of cytoplasmic microtubule subunits. *Proc. Natl. Acad. Sci. USA* 69:2890–2894.
7. Bradford, M. 1976. A rapid sensitive method for the quantitation of microgram quantities of protein utilizing the principle of protein-dye binding. *Anal. Biochem.* 72:248–254.
8. Bryan, J. 1974. Biochemical properties of microtubules. *Fed. Proc.* 33:152–157.
9. Carlier, M.-F. 1983. Kinetic evidence for a conformation change of tubulin preceding microtubule assembly. *J. Biol. Chem.* 258:2415–2420.
10. Carpenter, F. H., and K. T. Harrington. 1972. Intramolecular cross-linking of monomeric proteins and cross-linking of oligomeric proteins as a probe of quaternary structure. *J. Biol. Chem.* 247:5580–5586.
11. Clark, D. C., S. R. Martin, and P. M. Bayley. 1981. Conformation and assembly characteristics of tubulin and microtubule protein from bovine brain. *Biochemistry* 20:1924–1932.
12. Cleveland, D. W., M. A. Lopata, P. Sherline, and M. W. Kirschner. 1981. Unpolymerized tubulin modulates the level of tubulin mRNAs. *Cell* 25:537–546.
13. Condeelis, J., J. Salisbury, and K. Fugiwara. 1981. A new protein that gels F Actin in the cell cortex of *Dictyostelium Discoideum*. *Nature (Lond.)* 292:161–163.
14. Dietrich, H. W., and R. C. Williams, Jr. 1978. Reversible dissociation of the  $\alpha\beta$  dimer of tubulin from bovine brain. *Biochemistry* 17:3900–3907.
15. Durham, A. C. H. 1972. Structures and roles of the polymorphic forms of tobacco mosaic virus protein. I. Sedimentation studies. *J. Mol. Biol.* 67:289–305.
16. Durham, A. C. H., J. T. Finch, and A. Klug. 1971. States of aggregation of tobacco mosaic virus protein. *Nature New Biol.* 229:37–42.
17. Erikson, H. P. 1974. Assembly of microtubules from preformed, ring-shaped protofilaments and 6-S tubulin. *J. Supramol. Struct.* 2:393–411.
18. Fane, A. G., C. J. D. Fell, and A. G. Waters. 1981. The relationship between membrane surface pore characteristics and flux for ultrafiltration membranes. *J. Membr. Sci.* 9:245–262.
19. Gethner, J. S., G. W. Flynn, B. J. Berne, and F. Gaskin. 1977. Characterization of heterogeneous solutions using laser light scattering: study of the tubulin system. *Biochemistry* 16:5776–5780.
20. Gethner, J. S., G. W. Flynn, B. J. Berne, and F. Gaskin. 1977. Equilibrium components of tubulin preparations. *Biochemistry* 16:5781–5785.
21. Gilbert, G. A. 1959. Sedimentation and electrophoresis of interacting substances. I.

- Idealized boundary shape for a single substance aggregating reversibly. *Proc. R. Soc. Lond. A* 250:377-388.
22. Jeffrey, P. D. 1974. Polymerization behavior of bovine zinc-insulin at neutral pH. Molecular weight of the subunit and the effect of glucose. *Biochemistry* 13:4441-4446.
  23. Johnson, K. A., and G. G. Borisy. 1977. Kinetic analysis of microtubule self-assembly *in vitro*. *J. Mol. Biol.* 117:1-31.
  24. Keith, C. H., J. R. Feramisco, and M. Shelanski. 1981. Direct visualization of fluorescein-labeled microtubules *in vitro* and in microinjected fibroblasts. *J. Cell Biol.* 88:234-242.
  25. Laemmli, U. K. 1970. Cleavage of structural proteins during the assembly of the head of bacteriophage T4. *Nature (Lond.)* 227:680-685.
  26. Landis, E. M., and J. A. Pappenheimer. 1963. Exchange of substances through the capillary walls. In *Handbook of Physiology, Circulation II*. Philip Dow, editor. Waverly Press, Inc., Baltimore, MD. 961-1034.
  27. Lauffer, M. A. 1975. Entropy-driven processes in biology. Polymerization of tobacco mosaic virus protein and similar reactions. In *Molecular Biology, Biochemistry and Biophysics*. No. 20. Springer-Verlag, New York.
  28. Lauffer, M. A., and C. L. Stevens. 1968. Structure of the tobacco mosaic virus particle: polymerization of the tobacco mosaic virus protein. *Adv. Virus Res.* 13:1-63.
  29. Lee, J. C., and S. N. Timasheff. 1977. *In vitro* reconstitution of calf brain microtubules: effects of solution variables. *Biochemistry* 16:1754-1764.
  30. Lee, J. C., R. P. Frigon, and S. N. Timasheff. 1973. The chemical characterization of calf brain microtubule protein subunits. *J. Biol. Chem.* 248:7253-7262.
  31. Lowry, O. H., N. J. Rosebrough, L. A. Farr, and R. J. Randall. 1951. Protein measurement with the folin phenol reagent. *J. Biol. Chem.* 193:265-275.
  32. Ludueña, R. F., E. M. Shooter, and L. Wilson. 1977. Structure of the tubulin dimer. *J. Biol. Chem.* 252:7006-7014.
  33. MacLean-Fletcher, S. O., and T. O. Pollard. 1980. Viscometric analysis of the gelation of *Acanthamoeba* extracts and purification of two gelation factors. *J. Cell Biol.* 85:414-428.
  34. Mandelkow, E.-M., A. Harmensen, E. Mandelkow, and J. Bordsas. 1980. X-ray kinetic studies of microtubule assembly using synchrotron radiation. *Nature (Lond.)* 287:595-599.
  35. Marcum, J. M., and G. G. Borisy. 1978. Characterization of microtubule protein oligomers by analytical ultracentrifugation. *J. Biol. Chem.* 253:2825-2833.
  36. Marcum, J. M., and G. G. Borisy. 1978. Sedimentation velocity analyses of the effect of hydrostatic pressure on the 30S microtubule protein oligomer. *J. Biol. Chem.* 253:2852-2857.
  37. Margolis, R. L., and L. Wilson. 1979. Regulation of the microtubule steady state *in vitro* by ATP. *Cell* 18:673-679.
  38. Morrow, J. S., and V. T. Marchesi. 1981. Self-assembly of spectrin oligomers *in vitro*: a basis for a dynamic cytoskeleton. *J. Cell Biol.* 88:463-468.
  39. Morrow, J. S., D. W. Speicher, W. J. Knowles, J. C. Hsu, and V. T. Marchesi. 1980. Identification of functional domains of human erythrocyte spectrin. *Proc. Natl. Acad. Sci. USA* 77:6592-6596.
  40. Okada, Y., and T. Ohno. 1972. Assembly mechanism of tobacco mosaic virus particle from its ribonucleic acid and protein. *Mol. Gen. Genet.* 114:205-213.
  41. Olmstead, J. B. 1981. Tubulin pools in differentiating neuroblastoma cells. *J. Cell Biol.* 89:418-423.
  42. Oosawa, F., and S. Asakura. 1975. Thermodynamics of the Polymerization of Protein. Academic Press, Inc., New York.
  43. Palmer, G. R., D. C. Clark, P. M. Bayley, and D. B. Satelle. 1982. A quasi-elastic light scattering study of tubulin and microtubule protein from bovine brain. *J. Mol. Biol.* 160:641-658.
  44. Pantaloni, D., M. F. Carlier, C. Simon, and G. Batelier. 1981. Mechanism of tubulin assembly: role of rings in the nucleation process and of associated proteins in the stabilization of microtubules. *Biochemistry* 20:4709-4716.
  45. Prakash, V., and S. N. Timasheff. 1983. The interaction of vincristine with calf brain tubulin. *J. Biol. Chem.* 258:1689-1697.
  46. Regula, C. S., J. R. Pfeiffer, and R. D. Berlin. 1981. Microtubule assembly and disassembly at alkaline pH. *J. Cell Biol.* 89:45-53.
  47. Rodbard, D., and A. Chrambach. 1971. Estimation of molecular radius, free mobility, and valence using polyacrylamide gel electrophoresis. *Anal. Biochem.* 40:95-134.
  48. Salmon, E. D. 1975. Pressure-induced depolymerization of spindle microtubules. II. Thermodynamics of *in vivo* spindle assembly. *J. Cell Biol.* 66:114-127.
  49. Scheele, R. B., and G. G. Borisy. 1978. Electron microscopy of metal-shadowed and negatively stained microtubule protein. Structure of the 30S oligomer. *J. Biol. Chem.* 253:2846-2851.
  50. Schizuta, Y., H. Shizata, M. Gallo, P. Davies, I. Pastan, and M. S. Lewis. 1976. Purification and properties of filamin, an actin binding protein from chicken gizzard. *J. Biol. Chem.* 251:6562-6567.
  51. Sloboda, R. D., W. L. Dentler, R. A. Bloodgood, B. R. Telzer, S. Granett, and J. L. Rosenbaum. 1976. Microtubule-associated proteins (MAPs) and the assembly of microtubules *in vitro*. *Cold Spring Harbor Conf. Cell Proliferation* 3(Book C):1171-1212.
  52. Stearns, M. E., and D. L. Brown. 1979. Purification of a microtubule-associated protein based on its preferential association with tubulin during microtubule initiation. *FEBS (Fed. Eur. Biochem. Soc.) Lett.* 101:15-20.
  53. Stephens, R. E. 1975. High-resolution preparative SDS-polyacrylamide gel electrophoresis: fluorescent visualization and electrophoresis elution-concentration of protein bands. *Anal. Biochem.* 65:369-379.
  54. Stossel, T. P., and J. H. Hartwig. 1975. Interactions between actin, myosin and an actin-binding protein from rabbit alveolar macrophages. *J. Biol. Chem.* 250:5706-5712.
  55. Tilney, L. G. 1975. Actin filaments in the acrosomal reaction of *Limulus* sperm. Motion generated by alterations in the packing of the filaments. *J. Cell Biol.* 64:289-310.
  56. Weisenberg, R. C., G. G. Borisy, and E. W. Taylor. 1968. The colchicine-binding protein of mammalian brain and its relation to microtubules. *Biochemistry* 7:4466-4479.
  57. Weisenberg, R. C., and S. N. Timasheff. 1970. Aggregation of microtubule subunit protein. Effects of divalent cations, colchicine, and vinblastine. *Biochemistry* 9:4110-4116.
  58. Weisenberg, R. C. 1980. Role of co-operative interactions, microtubule associated proteins and guanosine triphosphate in microtubule assembly: A model. *J. Mol. Biol.* 139:660-677.
  59. Zarling, D. A., A. Watson, and F. H. Bach. 1980. Mapping of lymphocyte surface polypeptide antigens by chemical cross-linking with BSOCOES. *J. Immunol.* 129:913-920.